Journal of
Marine Science and Engineering

MDPI

Article

Study of Intensive Anthropogenic Impacts of Submerged Wastewater Discharges on Marine Water Areas Using Satellite Imagery

Valery Bondur and Viktor Zamshin *

AEROCOSMOS Research Institute for Aerospace Monitoring, 105064 Moscow, Russia
* Correspondence: viktor.v.zamshin@gmail.com

Abstract: This paper focuses on a detailed analysis of coastal waters under the conditions of the intense anthropogenic impacts of submerged wastewater discharges, using optical and radar satellite images. The features of the intense anthropogenic impacts on the coastal waters of the northern part of the Black Sea were studied, based on the processing and analysis of systematized archival satellite and sea truth data (2015–2021). Techniques based on the formation and analysis of the spatial (2-dimensional) spectra of optical and radar satellite images, normalized radar cross-section (NRCS), and the normalized spectral index are proposed. It is convincingly shown that these techniques make it possible to register and interpret the changes in the spatial structure of wind waves, as well as the changes in the optical spectral characteristics caused by submerged wastewater discharge due to the complex hydrodynamic and hydro-optical impact. A comprehensive analysis of the results of the processing of the heterogeneous satellite and sea truth data was carried out using a geographic information system. It was found that surface disturbances caused by anthropogenic impacts due to submerged wastewater discharges were detected by local "quasi-monochromatic" spectral maxima caused by the generation of short-period internal waves (wavelengths from ~30 m to ~165 m). These maxima can be registered by high-resolution optical and radar imagery. NRCS anomalies (2–4 dB contrasts), due to the surfactant films, floating jets, and turbulence related to wastewater discharge, are registered and described, as are the changes in the spectral radiance distributions in the blue and green bands of the electromagnetic spectrum.

Keywords: satellite remote sensing; coastal waters; wastewater discharge; anthropogenic impacts; comprehensive monitoring; spatial spectra; multispectral data; radar data

check for updates

Citation: Bondur, V.; Zamshin, V. Study of Intensive Anthropogenic Impacts of Submerged Wastewater Discharges on Marine Water Areas Using Satellite Imagery. *J. Mar. Sci. Eng.* **2022**, *10*, 1759. https://doi.org/10.3390/jmse10111759

Academic Editor: Milva Pepi

Received: 30 September 2022
Accepted: 10 November 2022
Published: 15 November 2022

1. Introduction

One of the most urgent problems in the sphere of environmental protection is the pollution of marine areas, particularly the coastal ones. More than half of the world's population lives in coastal regions; so, they are subjected to intense anthropogenic impacts [1]. Among the main sources of such impacts are the industrial and domestic effluents discharged directly into the sea, substances used in agriculture and forestry, spills due to shipboard works, accidents in maritime transport and pipelines, etc., and wastewater discharges have the most significant impact on the ecosystems of coastal waters [1,2].

To solve this problem, it is promising to apply satellite methods, which have ample opportunities, including [3] a wide range of survey; the quick delivery of data; the capability to work in any hard-to-reach areas of the seas and oceans; the possibility to obtain information with different spatial and temporal resolutions in different bands of the electromagnetic spectrum; a wide range of recorded parameters of the water environment; and highly reliable data. The efficiency of these methods increases significantly if they are combined with the results of ground truth measurements (see, e.g., [4,5]) and modeling results (see, e.g., [4,6–8]).

The use of satellite methods to study the intensive anthropogenic impacts on the seas and oceans is based on the fact that as a result of both the direct and the indirect influence of the various processes occurring in the water environment under such impacts, the parameters of the physicochemical and biological fields of the seas and oceans change in terms of hydrodynamics, turbidity, temperature, spectral radiance, dielectric permittivity, salinity, concentrations of the biogenic elements (nitrogen, oxygen, phosphorus), acidity, heavy metal concentrations, phytoplankton conditions, etc. [3,4]. They lead to a change in the characteristics of the signals recorded by various types of remote sensing equipment [3,6].

To register such changes, both optical [3,4,9–11] and radar [3,6,12] remote sensing assets can be used. Furthermore, the most effective methods are those based on the combined use of satellite data generated in different bands of the electromagnetic spectrum [3,4,13,14].

Detecting and studying the anthropogenic impacts on marine areas using satellite data are complicated by the fact that other processes and phenomena can also cause changes in the parameters of the physicochemical and biological fields. Such processes and phenomena include, for example, wind calm areas, atmospheric internal waves and vortices, convective cells, upwelling, currents, algal blooms, bottom sediment detachment, natural hydrocarbon emissions succeeded by oil films on the sea surface, etc. [3,4,6,12,15–17].

In this paper, we address the features of the application of satellite methods for the study of coastal waters under the conditions of intense anthropogenic impacts using optical and radar imagery. The problem of generalization and the further deepening of knowledge in the field of the remote sensing of the intensive anthropogenic impacts on coastal waters is studied using the example of submerged wastewater discharges. Taking into account the results of the analysis of the current state of research in this field, approaches to the use of satellite data for the study of anthropogenic impacts on coastal waters (associated with wastewater discharges) are formulated. Taking into account the joint use of these approaches the research methodology is developed. In accordance with the proposed methodology, the water area of the northern part of the Black Sea is monitored using optical and radar satellite images of high (~1 m) and medium (~10 m) spatial resolution, and a set of sea truth data is also used. The innovative contribution of the article consists in the use of various methods of processing both single and multi-year time series of remote sensing images in order to study the mentioned thematic problem. An approach based on the analysis of the two-dimensional spectra of satellite optical and radar images is applied to identify anomalies in the spatial structure of the surface waves associated with the studied anthropogenic impacts, which are caused by submerged wastewater discharge. Specialized approaches to the analysis of the spatial distributions of the spectral radiance and NRCS of the sea surface are applied. One feature of the effort is a comprehensive analysis of the results of the processing of the heterogeneous satellite and contact data accumulated over an 8-year period using a geoinformational system. This analysis demonstrated the capabilities and potential of the modern remote sensing methods for detecting and studying anthropogenic impacts on coastal waters using the example of submerged wastewater discharge.

Below, we address three main approaches to the satellite study of anthropogenic impacts on coastal waters.

2. Approaches to a Methodology for Satellite Studies of Anthropogenic Impacts on Coastal Water Areas Due to Submerged Wastewater Discharges

2.1. Approach Based on the Spatial Spectral Analysis Using High- and Medium-Resolution Optical and Radar Satellite Imagery

An effective approach to revealing and studying the anthropogenic impacts on coastal water areas due to submerged wastewater discharges is the method based on the spatial (2-dimensional/2D) spectral analysis of satellite imagery. This method allows for the studying of the low-contrast structures caused by these impacts, which are manifested in changes in the spatial structure of surface waves [3,4]. At the same time, the anthropogenic impacts generate internal waves, turbulence, and films of surfactants. They cause distortion of the surface wave spatial spectra and can be registered using satellite imagery [3,4,6].

For example, in [4] it was shown that in the 2D spectra of high-resolution satellite images in the areas of submerged discharges, narrow spectral harmonics were revealed that corresponded to "quasi-monochromatic" (sometimes multimode) wave systems on the sea surface, with the lengths $\overline{\Lambda}$ = 30–200 m, which were also recorded by wave buoys [4]. An analysis of the physical mechanisms responsible for the appearance of these harmonics, performed using a spectral analysis of the depths of the isotherms measured by high-precision thermistor strings, showed that these effects were due to the manifestation of ultrashort internal waves generated by turbulent jets of submerged discharges in a stratified environment [4]. A detailed explanation of such effects, based on the results of a large amount of satellite, sea truth, and model data, is given in [3,4,6,18].

Here, we use and develop an approach to studying the anthropogenic impacts on coastal water areas related to submerged wastewater discharges using the results from the spatial spectral analysis of satellite imagery. The appropriate technique and the results obtained are discussed below.

2.2. Approach Based on the Registration of Changes in Normalized Radar Cross-Section of Sea Surface Using Radar Satellite Imagery

The approach consists in identifying anthropogenic impacts on coastal waters, including those associated with submerged wastewater discharges, by registering and analyzing NRCS contrasts using radar satellite images of the sea surface. The following main reasons for the appearance of such contrasts in the satellite radar images of the sea surface in anthropogenic impact areas are taken into account [3]:

- Changes in rough sea surface spectra in the areas of anthropogenic impact manifesting in attenuation (slicks) or amplification (rips) of surface waves;
- Doppler change in the frequency of registered radio signals when local currents appear due to manifestations of anthropogenic impacts on marine areas;
- Local changes in sea water dielectric permittivity due to various anthropogenic factors.

Here, first of all, we use the capabilities of radar satellite imagery to register changes in the spectral composition of surface waves, leading to changes in the NRCS because of the Bragg mechanism of radio wave scattering by the sea surface [3,19,20]. Here, we develop the approach to studying the anthropogenic impacts on marine areas due to wastewater discharges that is based on the analysis of the NRCS distributions registered in the radar satellite imagery.

2.3. Approach Based on the Analysis of Sea Surface Radiance Distributions Using Multispectral Satellite Imagery

Another physical mechanism that determines the capability of the remote indication of anthropogenic impacts on marine areas involves the changes in the hydro-optical characteristics of the water environment, i.e., changes in its radiance.

Among the main parameters of the water environment that are sensitive to pollution are the changes in the absorption and backscattering of light because of an increase in the concentration of suspended and dissolved substances [9–11]. Note that the spectral dependence of the backscattering index is proportional to λ^{-n}, where λ is the wavelength, and the index n is about 4.3 for pure water, and it is 0.4–2.2 for a high content of mineral or organic suspension [21]. Therefore, under conditions of anthropogenic impacts, when suspensions get into the water environment, the backscattering index of light will increase, which will lead to an increase in the radiance recorded by means of optical satellite.

The longwave radiation of the visible range of the electromagnetic spectrum (red region) penetrates into the water column to a much lesser depth compared to the shortwave radiation [21]. At the same time, the radiance of the sea surface in the shortwave part of the visible range of the electromagnetic wave spectrum (blue region) largely depends on the concentration of chlorophyll and the composition and concentration of dissolved organic substances [10,22]. Radiance in the green region of the spectrum is largely determined by the composition, concentration, and size distribution of suspended particles [21].

To detect such phenomena, multispectral and hyperspectral optical satellite imagery is used [3,4,14,16,17].

Thus, when studying the anthropogenic impacts due to effluents running into the water environment, one should expect significant contrasts in the radiance in the blue and green regions of multispectral optical images; this is discussed below.

3. Research Methodology and Data Used

3.1. General Flowchart of the Research Methodology

Figure 1 shows a general flowchart of the research methodology, taking into account the features of all the approaches discussed above. The colors of the rectangles in Figure 1 indicate various domains of data (optical, radar, sea truth, a priori, and comprehensive). At the same time, various data flows (optical and radar data of high and medium resolution and a priori and comprehensive data) are demonstrated using lines of different colors and types [3,4,10,13,18].

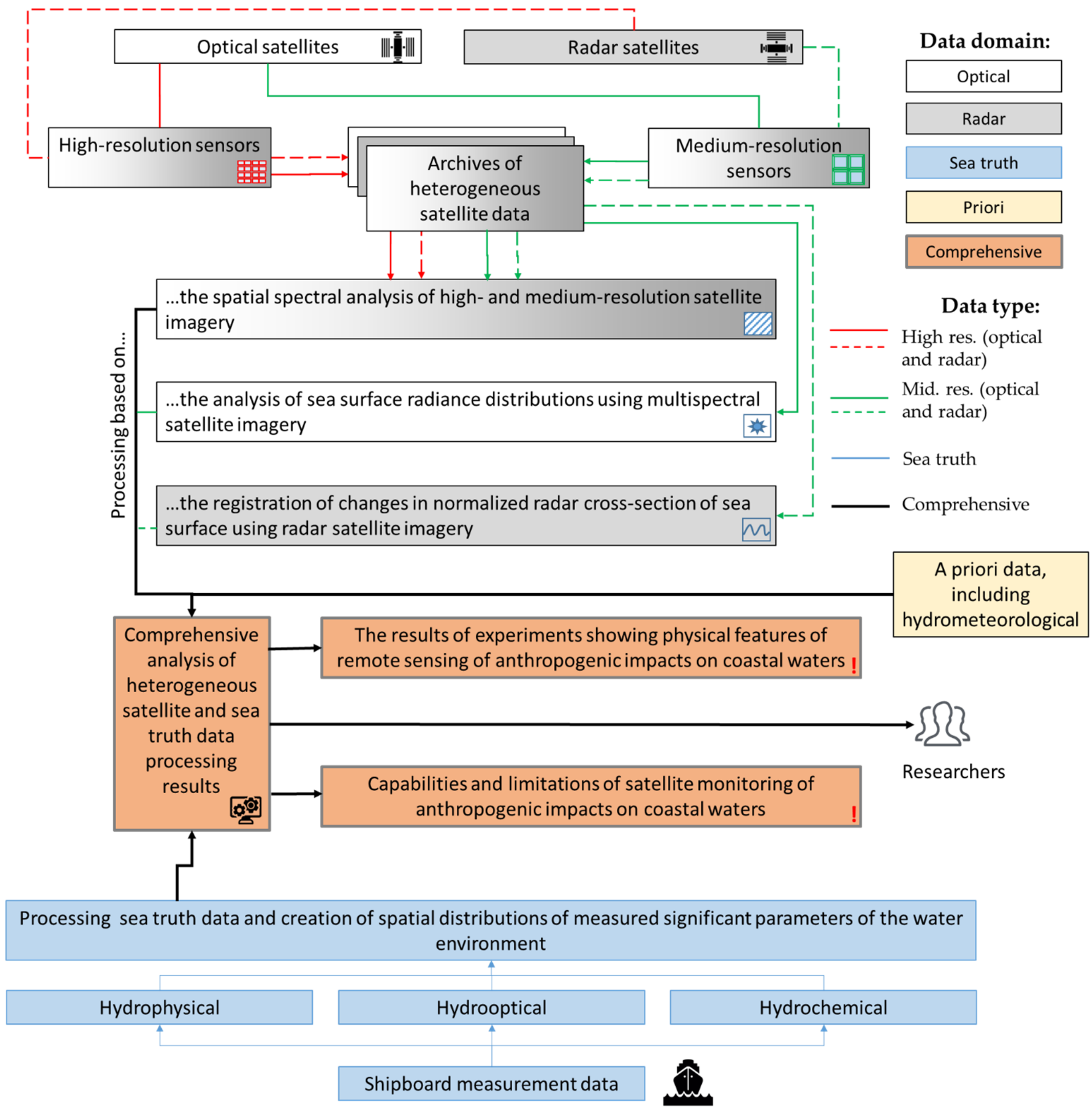

Figure 1. General flowchart of the research methodology.

The results of the processing of the heterogeneous satellite and the sea truth data processed using different approaches were comprehensively analyzed using a geoinformational system. In the course of such an analysis, a priori data were also used, including hydrometeorological parameters, information on the location of outfall collectors, specific flow rates, etc.

3.2. Research Methodology Based on the Analysis of Spatial Spectra of High- and Medium-Resolution Optical and Radar Satellite Imagery

The study carried out in this work of the impacts of submerged wastewater discharges on the spatial structure of sea waves is based on the analysis of the spatial spectra of high-resolution (1 m or less) satellite image fragments formed on a regular spatial grid (with, for example, a step of ~1 or ~2 km). Moreover, in this study, in addition to the approach already used in previous works [3,4], the studies of a long-term (annual) time series of medium-resolution (10 m) satellite images were carried out within fragments of ~5 km per side (see the flowchart in Figure 1).

The method made it possible to study the dynamics of the anthropogenic impacts, due to both seasonal and hydrometeorological factors, on the structure of sea waves. These parameters considerably affect the generation of internal waves by the wastewater jets [4].

The methodology flowchart is given in Figure 2. According to this methodology, for each processed fragment of a satellite image complex 2D spatial spectra were calculated, using the following equation [23]:

$$S\left(\nu_{n_x},\nu_{n_y}\right)=\sum_{n_x=0}^{N_x-1}\sum_{n_y=0}^{N_y-1}B\left(n_x,n_y\right)exp\left\{\frac{-2\pi i}{N}\left(\nu_{n_x}n_x+\nu_{n_y}n_y\right)\right\} \tag{1}$$

where ν_{n_x},ν_{n_y} are the spatial frequencies along the X and Y axes, respectively;

$N_x = N_y$ is the fragment's size;

$B(n_x,n_y)$ are the image radiance values.

Fast Fourier transform algorithms were used to speed up the computations [24].

Next, the 2D spatial spectra were transformed into power spectra on a logarithmic scale:

$$S_{lg}(\nu_{n_x},\nu_{n_y})=lg\left[\left|S(\nu_{n_x},\nu_{n_y})\right|^2\right] \tag{2}$$

The need for transformation (2) is explained by the fact that the Fourier spectra of sea surface images have a feature which is that the range of their changes in low- and high-frequency areas differs by several orders of magnitude.

Mosaics of the spatial spectra were synthesized and analyzed based on the results of the processing of the time series of satellite images. Solid arrows (see Figure 2) link the operations performed during the formation of the mosaics, using satellite image fragments selected on a regular spatial grid. The dashed arrows (see Figure 2) link the operations performed when generating the mosaics based on the time series of satellite images (a fragment with a fixed location was processed). The spatial spectra of the satellite images obtained and presented as mosaics were studied to identify the specific changes in these spectra corresponding to the surface manifestations of the anthropogenic impacts.

For the selected features of the spatial spectra, which consisted of the generation of additional spectral maxima related to the surface manifestations of the anthropogenic impact on marine areas due to submerged wastewater discharges, the spatial frequency was measured. The maximum (Nyquist) frequency in the 2D spectra was determined using the following equation [25]:

$$\nu_{\max}=\frac{1}{2\cdot R}, \tag{3}$$

where R is the pixel size.

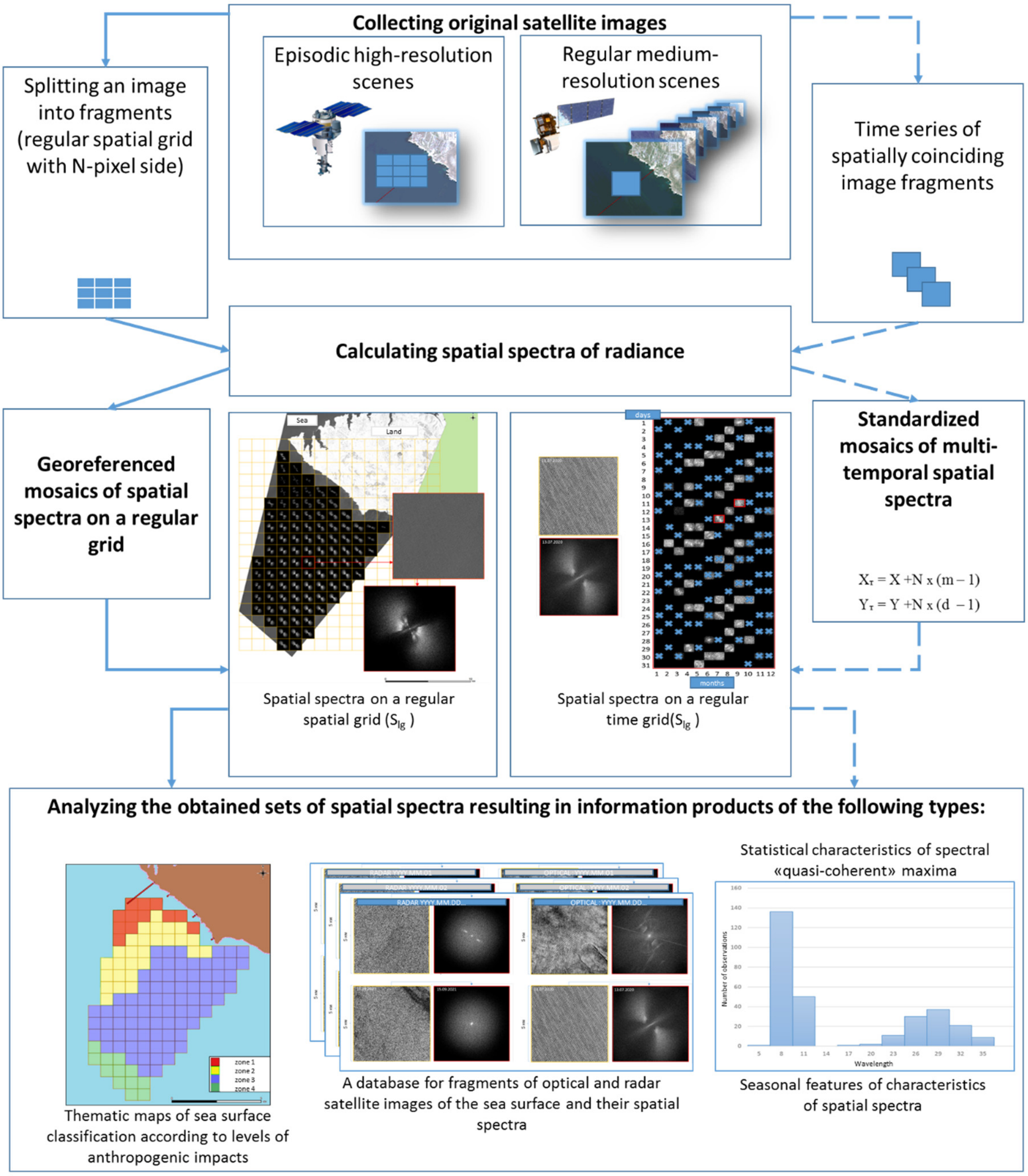

Figure 2. A flowchart of research methodology based on the analysis of spatial spectra of high- and medium-resolution optical and radar satellite imagery to study anthropogenic impacts on coastal water areas.

Due to the symmetry of the spectrum, the magnitude of the increment of the spatial frequency per pixel of the digital image of the spatial spectrum is:

$$\Delta\nu = \nu_{\max}/(0.5 \cdot N) \tag{4}$$

where $N = N_x = N_y$ is the image fragment size (in pixels).

The processing was performed using two modes, namely:

1. The spatial scanning mode (the studied image fragments are distributed in space), using high-resolution (~1 m) panchromatic optical and radar images;

2. Time scanning mode (the same water area region influenced by wastewater plumes is studied), using a long-term time series of medium-resolution (~10 m) optical and radar data.

A feature of such processing is the increased probability of observing the effects related to the anthropogenic impacts on marine areas. This was ensured by numerous time-distributed observations, some of which had been performed under favorable hydrometeorological conditions.

High-resolution (Pesurs-P, archive) and medium-resolution (Sentinel-2A/B [26]) optical imagery was used as the initial data, as well as high-resolution (TerraSAR-X, archive) and medium-resolution (Sentinel-1A/B [27]) radar data. The research also involved Kanopus-B and Landsat-8 [28] data.

3.3. Research Methodology Based on NRCS Distributions Based on Radar Satellite Imagery

To reveal the effects of the anthropogenic impacts caused by submerged wastewater discharges, in this work a technique was used that suggested the identification in the radar satellite imagery of the sea NRCS changes due to the anthropogenic impacts associated with discharges.

During the processing of the radar satellite images of the sea surface, the following data were recorded:

- NRCS contrast of the sea surface in the anomalous areas related to the anthropogenic and natural impacts against the background [3,6,29];
- Features of the shape, size, irregularity of the boundaries, and textural properties of these anomalous areas [15,30];
- A priori data, including locations of possible sources of natural and anthropogenic NRCS changes (including outfalls) [3,4,31];
- Hydrometeorological conditions, including near-surface wind velocity and direction, current characteristics, precipitation, etc. [6,13].

Furthermore, the classification of the studied anomalous areas with NRCS changes was carried out. The classification of such changes, as given in Figure 3, was taken into account. It is based on approaches to the study of the areas of the sea surface NRCS changes proposed in [6,15,29]. At the same time, the fact that the anthropogenic impacts caused by submerged wastewater discharges can lead to the formation of both film and non-film slicks (sea wave smoothing areas) [3,6], as well as rips, was taken into account.

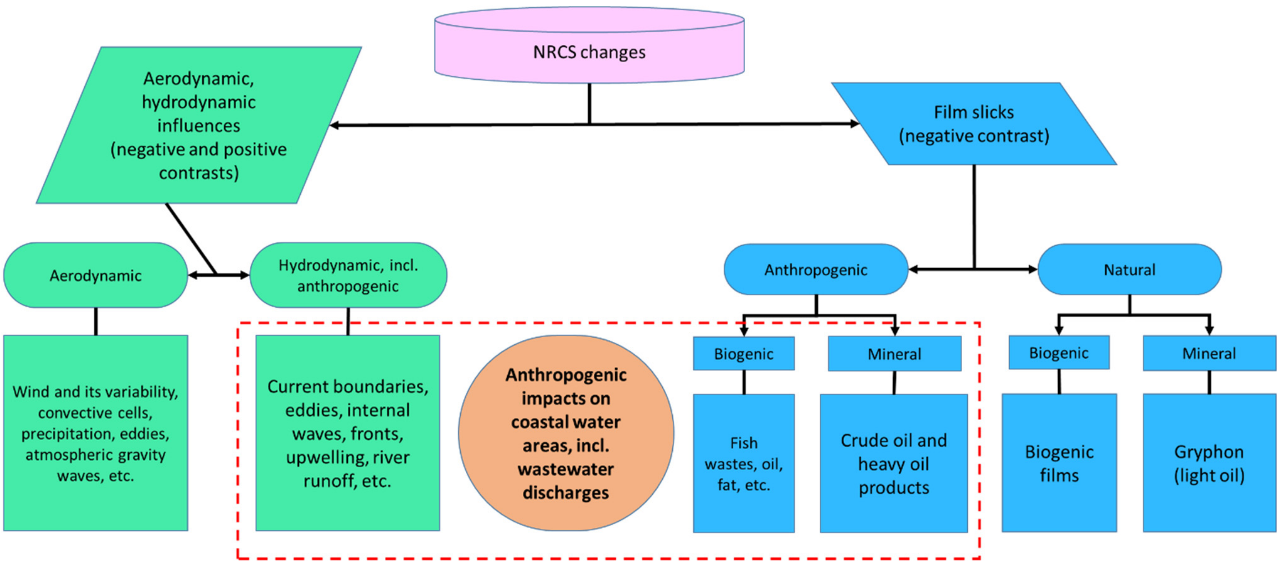

Figure 3. Classification of areas with NRCS changes which was used for revealing anthropogenic impacts on coastal water areas (the red outline shows phenomena of interest).

The time series of sea surface radar Sentinel-1A/B images covering the area affected by wastewater discharges were used as the initial data. During the analysis of these data, the approach described above was used. At the same time, additional a priori data on the location of the outfall collectors and hydrometeorological conditions were applied.

For the cases when the clear NRSCS contrasts due to anthropogenic impacts were revealed, color-coded NRCS maps were created. Conditional threshold levels corresponding to "moderate" and "intensive" anthropogenic impact were determined based on the analysis of such color-coded NRCS maps. The data obtained were generalized [4,13], which resulted in a decision as to whether the area under analysis with NRCS contrast was a surface manifestation of anthropogenic impacts because of wastewater discharges.

3.4. Research Methodology Based on the Analysis of Sea Surface Spectral Radiance by Multispectral Satellite Imagery

To study the anthropogenic impacts on coastal waters using multispectral satellite images, an approach based on the analysis of the time series of sea surface spectral radiance distributions was used. This informative parameter is usually used to assess the type of sea waters and their biological productivity (see, for example, [16,32]), to detect areas of water pollution (see, for example, [10]), and to study frontal zones, current fields, eddies, mixing zones, upwelling, etc. [3,33].

The methodology for studying the anthropogenic impacts on marine areas because of submerged wastewater discharges using multispectral satellite images is based on an approach that involves radiance variability in different parts of the electromagnetic spectrum [10,11]. Taking into account the physical features of such images, the proposed method used color indices calculated by the following equation [11,18]:

$$I_{GB} = G \times B, \tag{5}$$

where G is the spectral radiance in the green band of the electromagnetic spectrum, and B is the spectral radiance in the blue band.

Obviously, the absolute I_{GB} values depend not only on the optical characteristics of the near-surface water column, but also on the characteristics of the sea waves, the lighting conditions during imaging, the calibration characteristics of the equipment used, etc. [11,33]. Thus, in order to provide an adequate comparative analysis of I_{GB} spatial distributions obtained under different conditions, they were normalized to the level of background values, obtaining a normalized color index I_{GBnorm} [11,18]:

$$I_{GBnorm} = \frac{G_i \times B_i}{\sum\limits_{j=1}^{n} (G_j \times B_j)/n} \tag{6}$$

where G_i and B_i are the spectral radiances in the green and blue bands, respectively, for (i) pixels of multispectral images under processing; n is the number of pixels of the (j) background water area (out of wastewater plume) used for normalizing.

Here, we used a long-term time series of optical multispectral Sentinel-2A/B images (540 scenes) obtained over the period from 2015 to 2021. During the processing of multispectral satellite images, zones of intense anthropogenic impacts were identified, and their spatial and geometric characteristics were analyzed using sea truth hydrophysical, hydro-optical, and hydrochemical data.

4. Results and Discussion from Experimental Study

4.1. Results of the Analysis of Spatial Spectra of Satellite Images in the Zones of Anthropogenic Impacts on Marine Areas

Figure 4 shows example areas of the distribution of anomalies caused by anthropogenic impacts on coastal waters due to submerged wastewater discharges, revealed through the spatial spectral processing of high-resolution satellite images. The processing was carried out according to the methodology described in Section 3.2. During such processing, the spatial spectra of fragments of satellite images using a regular spatial grid revealed their characteristic changes corresponding to surface manifestations of anthropogenic impacts.

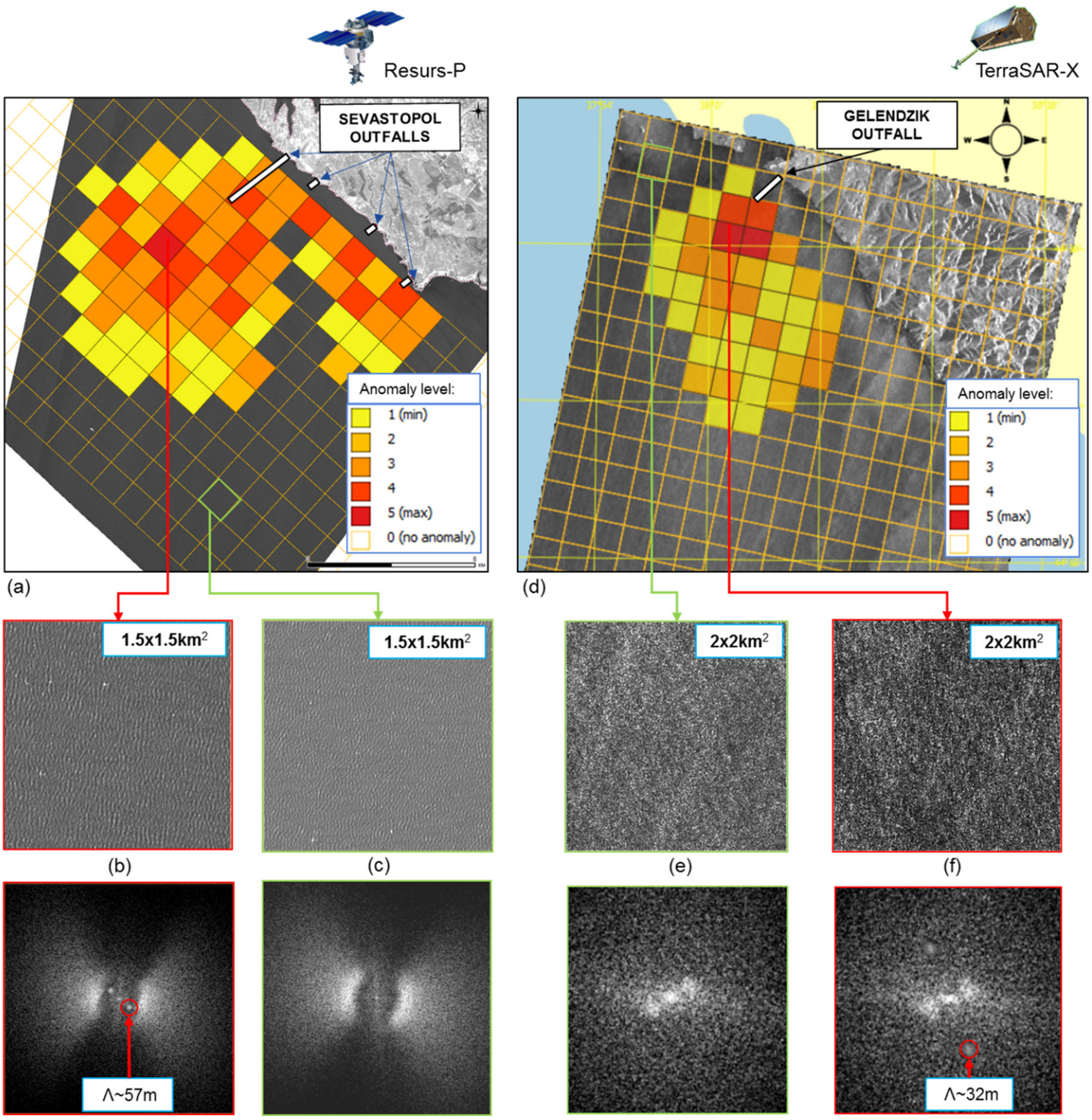

Figure 4. Example results from spatial spectral processing of high-resolution satellite images: (**a**) optical panchromatic Resurs-P No. 1 image of the region of Sevastopol; (**d**) TerraSAR-X radar image for the region of Gelendzhik. Fragments of original satellite images and corresponding 2D spatial spectra in the areas of effluent of submerged discharge (**b**,**f**) and in background areas (**c**,**e**).

Figure 4 (left) shows the processing result for the ~1 m panchromatic optical Resurs-P image of the northern part of the Black Sea (near the city of Sevastopol) in the vicinity of four outfalls. Figure 4a gives the original satellite image overlaid with a map with the spatial distribution of fragments classified as anomalous. The fragments were classified according to the intensity of additional "quasi-monochromatic" spectral harmonics in the spatial spectra of the processed image, caused by surface manifestations of short-period internal waves generated by submerged wastewater discharges [4]. The dark red color corresponds to the maximum level of anomaly manifestation and the light yellow to the minimum. The background fragments are not colored.

An analysis of Figure 4a shows that in the area of interest the zone of the manifestation of anthropogenic impacts due to the submerged plume is presented as two connecting areas confined to the locations of the four outfall collectors (white lines). The recorded manifestations of "quasi-monochromatic" spectral harmonics were found over a large area (up to 14 km from the coast). In this case, the most extended anomaly is confined to the collector of the main outfall, which has a length of ~3.3 km. The annual discharge is ~44 mln m^3/year. Moreover, manifestations of anomalies were also found near the collectors of minor discharge devices (annual discharges ~0.011 to ~1.095 mln m^3/year).

Figure 4 also shows example optical satellite image fragments and the corresponding 2D spatial spectra for the anomalous (Figure 4b) and background (Figure 4c) regions of the water area. In the example illustrated in Figure 4b, "quasi-monochromatic" spectral harmonics (meeting the condition $\Delta\Lambda << \overline{\Lambda}$) were revealed. The wavelengths corresponding to these harmonics were ~57 m with the width of the spectral maxima, $\Delta\Lambda$~7 m. The mechanisms for the occurrence of such "quasi-monochromatic" spectral harmonics, which are due to the generation of high-frequency internal waves and their interaction with surface waves in the zones of the manifestations of submerged discharges, are described in [4]. Such deformations of the spatial spectra were not detected in the background areas of the studied water area (see Figure 4c).

Figure 4 (right) shows the results of the spatial spectral processing of the high-resolution (~1 m) radar TerraSAR-X image of the northern part of the Black Sea in the area where the main outfall of the city of Gelendzhik is located. As in the case of the optical image processing, "quasi-monochromatic" spectral maxima were found in the two-dimensional spatial spectra of the fragments of the radar image in the zone of anthropogenic impacts due to submerged wastewater discharge (see Figure 4f). They indicate the presence of periodic spatial structures caused by surface manifestations of short-period internal waves generated by jets of submerged wastewater discharge. Such spectral maxima are not found in the background areas of the study area (see Figure 4e).

A map with the spatial distribution of anomalies identified based on the processing of a radar satellite image of coastal waters near the city of Gelendzhik is shown in Figure 4d (the symbols are the same as in Figure 4a). The most intense anomalies detected from the spatial spectra of the radar image fragments in this area corresponded to the surface manifestations of short-period internal waves with a length of $\overline{\Lambda}$~32 m ($\Delta\Lambda$~4 m). This is illustrated in Figure 4f.

An analysis of Figure 4d shows that the surface anomaly detected through the spatial spectral processing of a satellite radar image in the area of the outfall near the city of Gelendzhik has an elongated shape with dimensions of 14 × 18 km^2.

Thus, based on the results of the spatial spectral processing of the high-resolution optical and radar satellite images, the zones of the surface manifestations of the anthropogenic impacts caused by submerged wastewater discharges in the coastal waters near the cities of Sevastopol and Gelendzhik were identified, and their sizes were determined (from 5 to 18 km). These zones are detected by the "quasi-monochromatic" maxima in the spatial spectra of the image fragments, indicating the presence of quasi-periodic structures on the sea surface with spatial periods of the order of several tens of meters, due to the interaction of short-period internal waves, generated by submerged wastewater discharges, with surface waves [4].

Similar results were obtained earlier in experiments conducted in other water areas using high-resolution satellite images [3,4].

Figure 5 shows the results of the spatial spectral processing of medium-resolution (10 m) satellite images, performed according to the method described in Section 2.2, using a regular time grid.

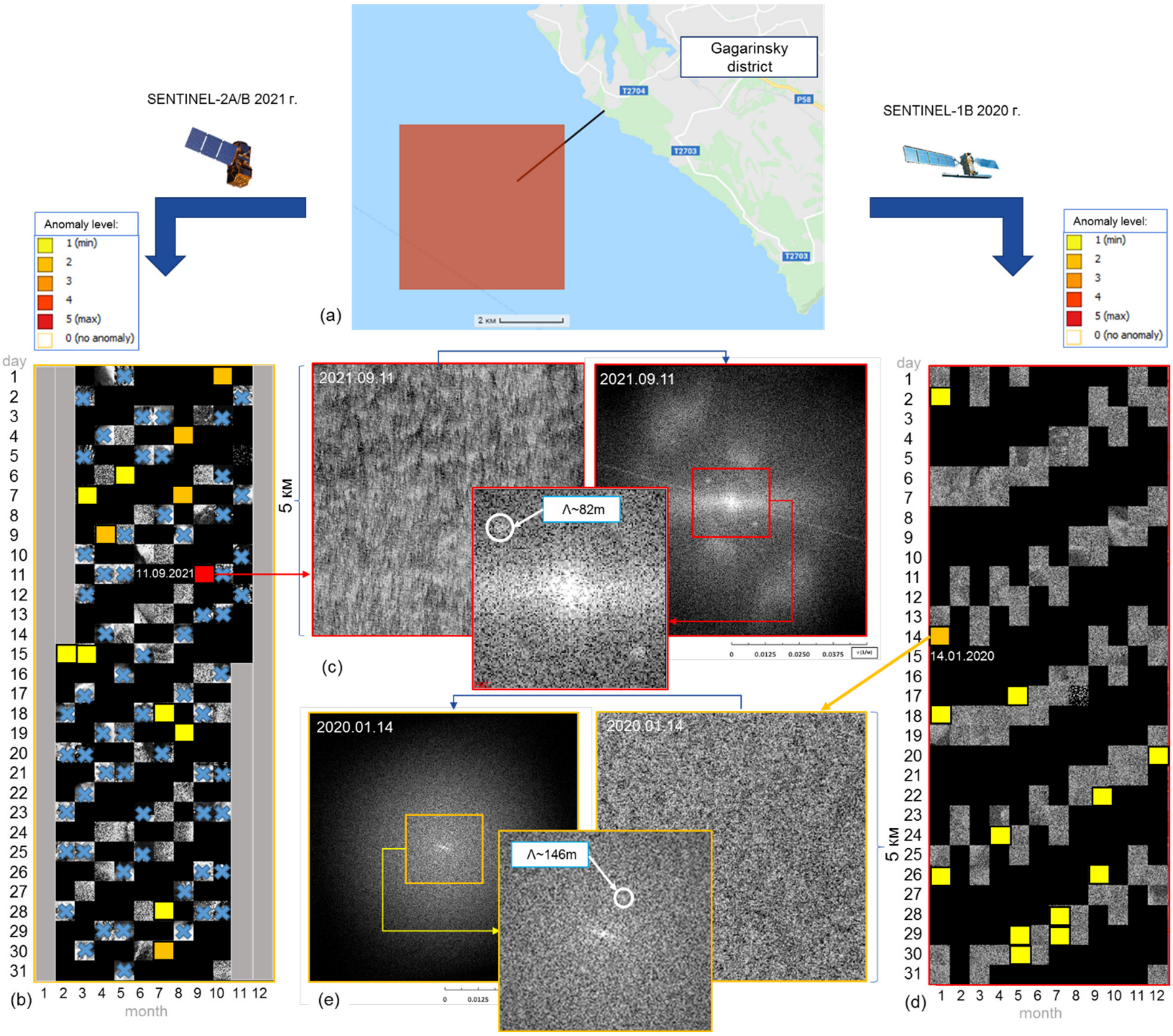

Figure 5. Example results of spatial spectral processing of medium-resolution satellite images, performed using a regular time grid: (**a**) the studied water area; (**b**,**d**) mosaics of fragments of multi-temporal images obtained by the Sentinel-2A/B multispectral camera (**b**) and the Sentinel-1B radar (**d**) with superimposed marks of detected anomalies (blue crosses—cloudiness); (**c**,**e**) example fragments of satellite images and their corresponding two-dimensional spatial spectra with the most intense manifestations of submerged wastewater discharge.

Figure 5b,d shows the mosaics obtained by the multispectral sensors of the Sentinel-2A/B satellites (Band no. 4, red) and the Sentinel-1B radar (VV polarization), respectively. These mosaics are based on the systematizing of the processed fragments of the multi-temporal satellite images of the study area by months and dates. The fragments that have "quasi-monochromatic" maxima in their spectra due to submerged wastewater discharges are marked with colors. Dark red corresponds to the maximum level of anomaly manifestation, light yellow to the minimum, and the blue crosses denote cloudiness. The time series of optical satellite images was obtained in the period from 15 February to 15 November 2021 (in the autumn–winter season the test area is characterized by almost permanent dense clouds). The time series of the radar satellite data was received in the period from 1 January to 31 December 2020.

An analysis of Figure 5b,d shows that by using the results of the spatial spectral processing of the time series of the medium-resolution optical and radar satellite images, a lot of dates were identified when the surface manifestations of anthropogenic impacts caused by submerged wastewater discharges were recorded. As in the examples shown in Figure 4 (spatial grid), these manifestations are expressed as "quasi-monochromatic" spectral maxima in the spatial spectra of the image fragments corresponding to the surface manifestations of internal waves with spatial periods of several tens of meters.

As an example, Figure 5c shows the results of the processing of an optical satellite image obtained on 11 September 2021. In the spatial spectrum of the selected image fragment, "quasi-monochromatic" spectral maxima corresponding to an internal wavelength of $\overline{\Lambda}$~82 m were revealed.

Figure 5e shows the results of the processing of a radar satellite image obtained on 14 January 2020 (in the spatial spectrum, "quasi-monochromatic" maxima corresponding to an internal wavelength of $\overline{\Lambda}$~146 m were revealed).

A comprehensive analysis of the abovementioned results of the spatial spectral processing of the high- and medium-resolution optical and radar satellite images will be carried out below in Section 4.4.

4.2. Results from Analysis of NRCS Distributions in the Zones of Anthropogenic Impacts on Sea Water Areas Based on Radar Satellite Imagery

According to the methodology presented in Section 3.3, the processing of the archival radar Sentinel-1A/B images of the coastal waters in the northern part of the Black Sea was carried out. As a result of the processing, the surface manifestations of anthropogenic impacts on coastal waters caused by submerged wastewater discharges were revealed. Example manifestations of such anthropogenic impacts in the radar satellite images are shown in Figure 6. This figure (left) shows example fragments of the original radar satellite images of the coastal waters in the zones of anthropogenic impacts near the cities of Gelendzhik and Sevastopol. At the right of this figure, the maps of the zones of reduced NRCS values corresponding to the original fragments are shown, demonstrating the spatial distribution of the anthropogenic impacts because of wastewater discharges.

An analysis of Figure 6 shows that the zones of the anthropogenic impacts of the submerged wastewater discharges (parts of the radar images with negative NRCS contrasts) found as a result of the processing are characterized by confinement to the discharge collectors. The studies used two grades of NRCS anomalies (see Figure 6)—"moderate" (yellow color, ~2 dB contrast against the background) and "strong" (red color, ~4 dB contrast against the background).

Figure 6a reveals that the strong NRCS anomalies (see red regions) are observed in the area of the outfall near the city of Gelendzhik, as well as in the seaward part of the water area adjacent to the outfall. The zone of moderate anomalies surrounds the zone of strong anomalies. Thus, the total size of the anthropogenic impact zone in the example reaches ~10 km in the direction from the coast to the open sea and ~4 km in the direction along the coast.

An analysis of Figure 6b shows that the NRCS anomalies in the area of outfalls near the city of Sevastopol (red areas) look like isolated spots bordered by moderate NRCS anomalies (yellow areas). Moreover, the NRCS anomalies are observed at various distances from the main and minor outfall collectors. The highest concentration of zones of anthropogenic impacts, identified by the radar images, was revealed directly at the head of the main outfall collector in Sevastopol.

The total size of the anthropogenic impact zone reaches ~8 km from the coast to the open sea and ~16 km along the coast. The significant length of the anthropogenic impact zone along the coast is due to the combined action of several outfalls.

The observed NRCS anomalies were due to a change in the spectral composition of the wind waves, which manifests itself in a decrease in the intensity of its gravitational-capillary component, which is responsible for the formation of the radar signal backscattering [3,6].

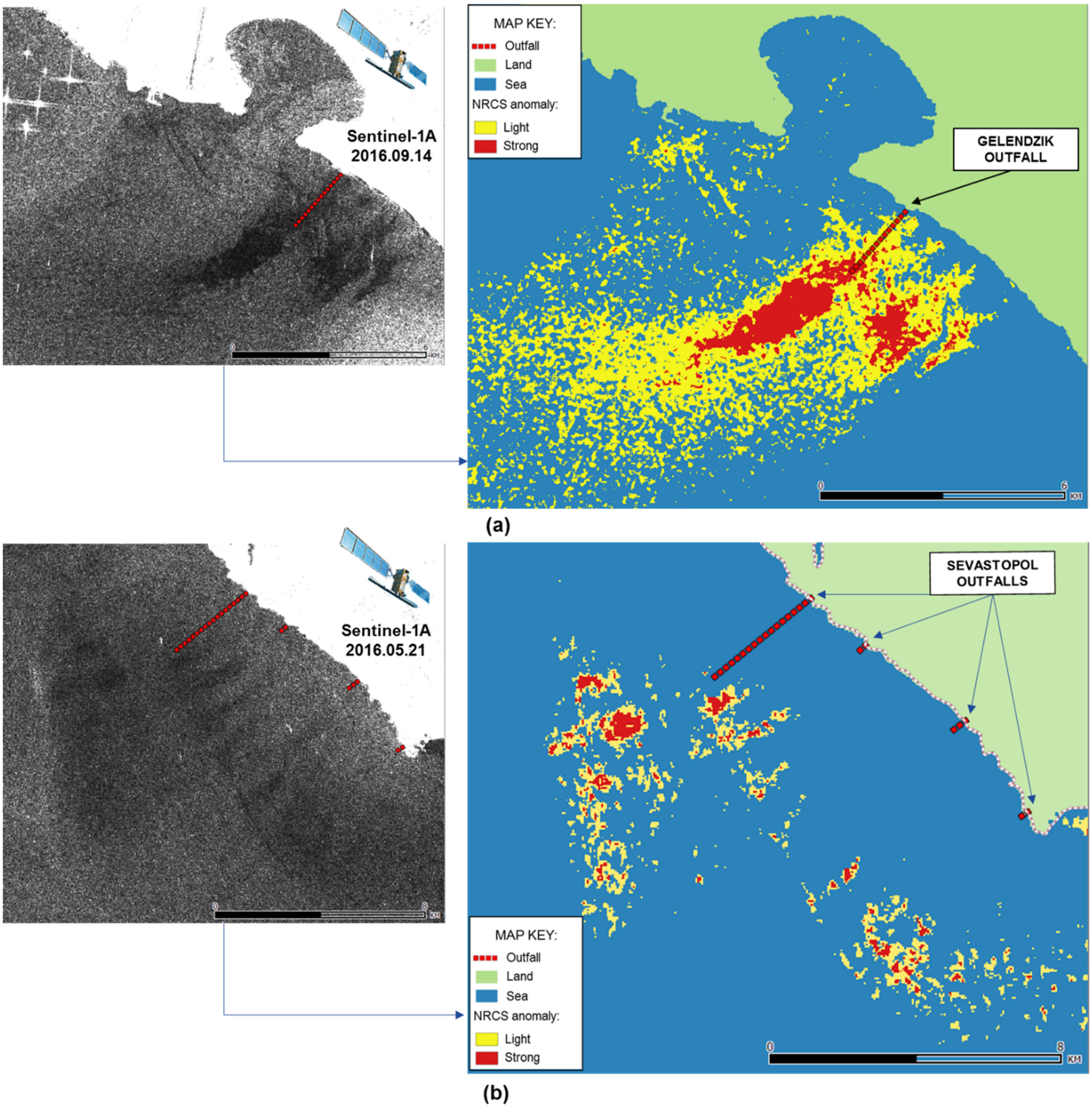

Figure 6. Example processing results for the radar Sentinel-1A image of coastal waters in the northern part of the Black Sea: near the city of Gelendzhik, 21 May 2016 (**a**), and near the city of Sevastopol, 14 September 2016 (**b**).

4.3. Results from Analysis of Spectral Radiance in the Areas of Anthropogenic Impacts on Marine Water Areas According to Multispectral Satellite Imagery

The methodology of the multispectral optical satellite imagery processing is given in Section 2.2. In the framework of this effort, the methodology was applied to the long-term time series of the multispectral Sentinel-2A/B images for the water area near the city of Sevastopol.

In total, 540 images obtained within the study area of interest in the period from 2015 to 2021 were systematized and processed. During this period, the main outfall collector near the city of Sevastopol functioned in an emergency mode, while the discharge was carried out through both the main outlet located at a distance of ~3.3 km from the coast at a depth of ~80 m and a collector rupture located at a distance of ~0.7 km from the coast at a depth of ~30 m [13,18]. Such conditions created physical prerequisites for the frequent ascent of a jet of discharge plume coming from an emergency rupture.

Figure 7a–c shows example calculation results for the spatial distributions of the normalized color index I_{Gbnorm} for the cases of registration of wastewater plumes coming from an emergency rupture on certain days of 2017, 2018, and 2019, respectively. In these examples, the I_{Gbnorm} spatial distributions are visualized in grayscale overlaying the vector data on the location of the outfall collector and the location of its emergency rupture.

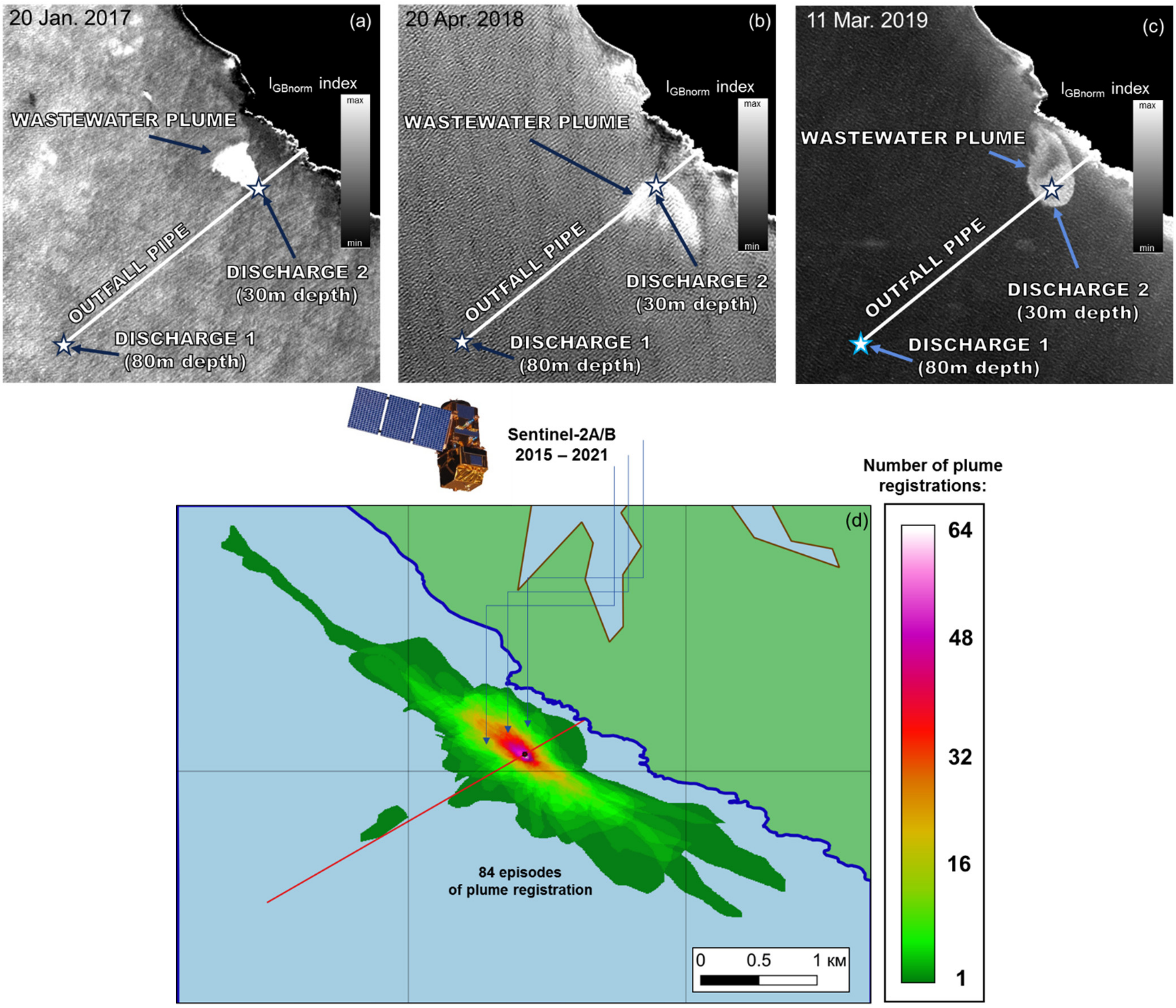

Figure 7. Example spatial distributions of normalized color index, I_{Gbnorm} (SENTINEL-2A/B): (**a**) 20 January 2017; (**b**) 20 April 2018 г.; (**c**) 11 March 2019 г.; (**d**) generalized map of plume registrations near Sevastopol, presented as a color-coded spatial distribution of a number of plume detection events.

An analysis of the examples of the spatial distributions of the I_{Gbnorm} normalized color index (Figure 7a–c) shows that the wastewater plume at the collector break appears as spots characterized by maximum levels of these index values.

In total, over the entire observation period (from 2015 to 2021), 84 cases of the registration of plumes coming from an emergency outfall rupture were identified. At the same time, no plume was observed near the main outlet of the discharge collector located at a considerable depth. This means that the effluents discharged to such a depth did not reach the near-surface layers as a concentrated jet. Therefore, there were no contrasts in the spectral radiance distributions recorded by the satellite methods.

A generalized map of plume registration results near Sevastopol, presented as a color-coded spatial distribution of a number of plume detection events, is given in Figure 7d. An analysis of Figure 7d showed that most cases (over 30) of the manifestations of wastewater plume were recorded directly at the location of the emergency rupture of the outfall collector. This means that cases of the almost vertical ascent of a jet of submerged discharge were most often recorded, which is consistent with the model concepts presented in [8].

4.4. Comprehensive Analysis

In the present study, a comprehensive analysis of the data obtained in the coastal waters near the city of Sevastopol was carried out. For this, a geoinformational system was used that combines heterogeneous satellite and sea truth data, as well as the results of their processing, within a single coordinate-time space.

Figure 8 illustrates cases of visually detectable surface manifestations of short-period internal waves in the zone of anthropogenic impacts of submerged wastewater discharges in satellite images obtained on 22 July 2015 from the Landsat-8 satellite (Figure 8a) and on 9 August 2019 from the Kanopus-V satellite (Figure 8b). The examples of visually detectable surface manifestations of short-period internal waves are superimposed on the results of the analysis of the spatial spectra of the high-resolution (1 m) image fragments, obtained on 17 April 2016 from the Resurs-P satellite.

In Figure 8a, clear surface manifestations of internal waves in the Landsat-8 image can be seen. These surface manifestations have the appearance of the typical signatures of internal waves, observed in the spatial distribution of the radiance field of the panchromatic band (15 m resolution) of the considered satellite image.

An analysis of Figure 8a shows that the locations of the surface manifestations of internal waves are generally confined to the outfall collector, while the wave crests are oriented mainly parallel to the coastline and cross, among other things, the zone of the registration of the intense manifestations of additional "quasi-monochromatic" spectral harmonics (dark red zone) identified in Section 4.1. The wavelength is approximately ~164 m.

Figure 8b illustrates a situation similar to that shown in Figure 8a. In this case, the detection of the surface manifestations of internal waves was performed using the Kanopus-V image (panchromatic band, 2.5 m resolution).

An analysis of Figure 8b indicates that the observed surface manifestations of an internal wave packet are confined directly to the end of the outfall collector and are located in the zone of anthropogenic impacts, identified earlier in Section 4.1 based on the spatial spectral processing of the Resurs-P data. The crests of the internal waves are oriented predominantly along the collector. The wavelength is approximately $\overline{\Lambda}$~90 m.

A comprehensive analysis of Figures 4b, 5 and 8 allows us to note that in the area of the outfall near the city of Sevastopol, anthropogenic impacts are observed as short-period internal waves (generated by an effluent jet). They have different directions of propagation (see the orientation of the spectral maxima in Figures 4b and 5, as well as the orientation of the crests of the internal waves in Figure 8).

It should be noted that the internal waves propagating along the coastline in the three considered examples (see Figures 4b, 5c and 8b) had a spatial period of less than 100 m. At the same time, the internal waves propagating along the coastline in both the considered examples (Figures 5e and 8a) had a spatial period of more than 100 m.

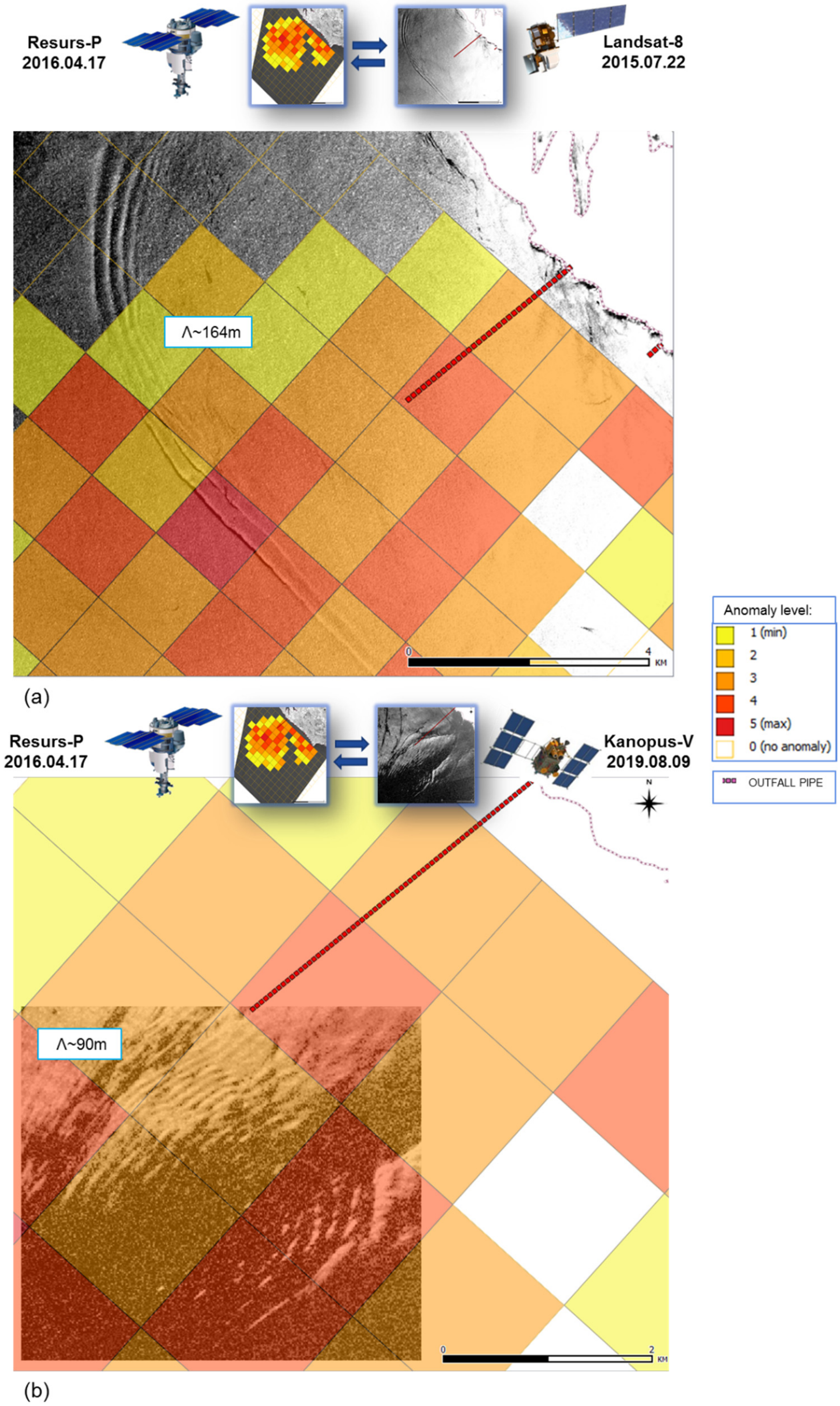

Figure 8. Example cases of visually detectable surface manifestations of internal waves ((**a**)–Landsat-8, (**b**)–Kanopus-V) in the area of submerged discharge impact detected as a result of the analysis of spatial spectra of the Resurs-P image in Sevastopol coastal water areas.

The different directions of the generated internal waves and the variations in their spatial periods can be explained by the variability of the hydrometeorological conditions (primarily currents) in combination with the variability of the operation modes of the outfalls. Apparently, the variability of the hydrometeorological conditions is also the essential factor causing the irregularity of the surface manifestations of the deep wastewater plumes (see Figure 5, which shows that the anomalies in the spectra of medium-resolution satellite images are detected inconsistently).

Figure 9 shows the results of the radar Sentinel-1A image (see Figure 6b) processing and the results of the spatial spectral analysis of the Resurs-P (see Section 4.1) image combined on a single map.

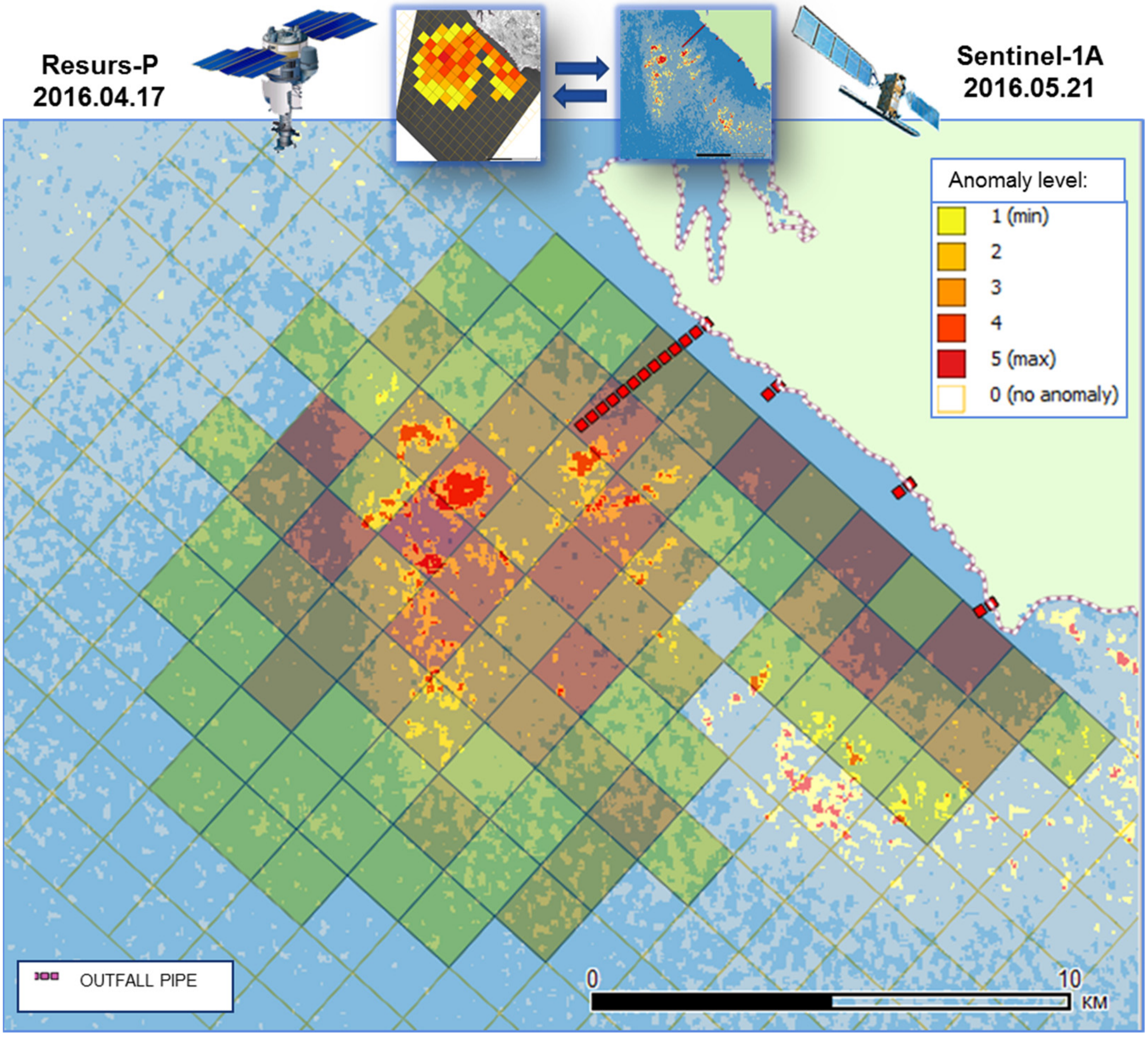

Figure 9. Example comparing the results of Sentinel-1A radar image processing and the results of the experiment on spatial spectral analysis of the optical Resurs-P image in the coastal waters of the city of Sevastopol.

An analysis of Figure 9 shows that the shape and spatial scales of the anthropogenic impacts of submerged wastewater discharges, recorded in the study area by various methods at different times, generally coincide. The shape of the zone of the manifestations of anthropogenic impacts is due to the several outfall collectors (the main one, ~3.3 km long, and the minor ones, much shorter).

The generalized analysis of the experimental results shown in Figures 4a, 5, 6b, 8 and 9 allows us to conclude that in the study area of the Black Sea near the city of Sevastopol, there is an extensive (~16 km long along the coast) zone of anthropogenic impacts due to wastewater discharge. Within this zone, the anthropogenic impacts manifested themselves as short-period internal waves propagating in various directions. Their surface manifestations can be recorded from high- and medium-resolution optical and radar satellite images. Moreover, the anthropogenic impacts due to submerged wastewater discharges manifest themselves in the changes in the intensity of the resonant component of the surface waves, as recorded by the satellite radars. Such changes are caused by surfactant films, deformation of the wave spectrum by the rising jet itself, and turbulence.

The data on the shape and location of the zone of anthropogenic impacts, as well as on the characteristics of the anthropogenic internal waves obtained by various methods, complement each other.

Let us analyze the effects recorded near the outlet, located at a distance of ~0.7 km from the coast at a depth of ~30 m. These effects (see Figure 7) are associated with the almost vertical ascent and further propagation of wastewater plumes in the near-surface layer of the water column. This is confirmed, on the one hand, by Figure 7 and, on the other hand, by the simulation results [8].

Figure 10 presents the example results of the comparison of the wastewater plume detection as a result of the processing satellite and the sea truth data obtained near the outfall at a distance of ~0.7 km from the coast. In this case, the set of outlines of the pollution zones (see Figure 10a) detected as a result of the analysis of the optical characteristics of the water environment using the I_{GBnorm} index (see Section 3.4) was considered as the results of the satellite multispectral image processing. The outlines of the pollution zones located to the northwest of the collector are green. The outlines of the pollution zones located to the southeast of the collector are red.

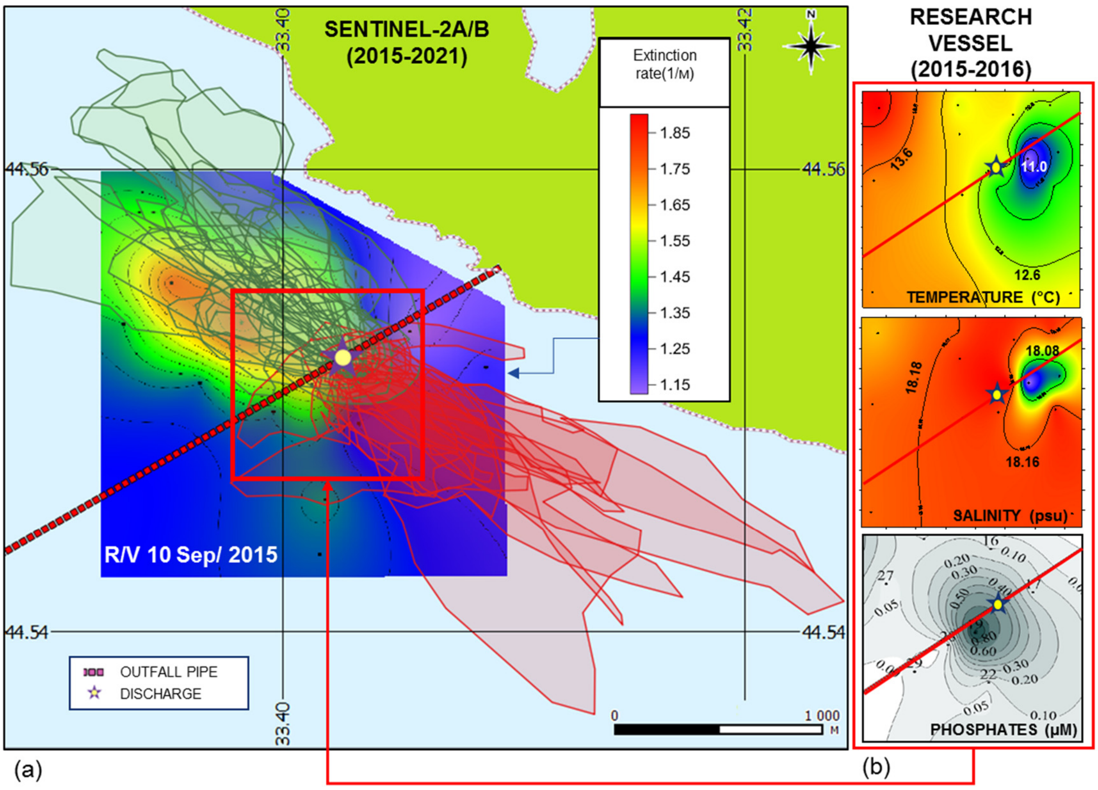

Figure 10. Example comparisons of wastewater plume detection results based on satellite and in situ data processing: (**a**) pollutions according to multispectral Sentinel-2A/B data superimposed on the map of spatial distribution of light attenuation index data; (**b**) example spatial distributions of the temperature, salinity, and phosphate content (shipborne data).

Thus, Figure 10 illustrates two typical modes of plume propagation. These modes depend on the currents.

Figure 10a shows the spatial distribution of the light attenuation index (“extinction rate”) in the layer of increased turbidity, obtained on 10 September 2015 as a result of ship data processing. On the right, in Figure 10b, there are examples of the spatial distributions of some significant parameters of the water environment, i.e., temperature, salinity, and phosphate content measured in the near-surface layer. The ship work was carried out between 2015 and 2016 aboard the R/V Biryuza [18].

An analysis of Figure 10a shows that the pollution zones caused by the inflow of effluents through the outfall rupture, as a rule, have an elongated shape and extend along the coast for distances of up to 1.5 km in both the southeast (red outlines) and in the northwest (green outlines) directions. The total length of the identified pollution zone reaches ~3 km, and the width is up to ~0.8 km. The distance from the coast to the place with the most frequent occurrence of pollution is ~0.7 km. At the same time, there is an adequate correspondence between the location of the northwestern “branch” of the pollution zone and the anomaly of the extinction rate recorded as a result of the shipborne measurements on 10 September 2015. The driving factors of the spatial variance of the plume are the stratification of the water environment and the characteristics of the background currents [6–8]. The test area is characterized by a bimodal regime of currents. As a result, there is a spread of pollution to the northwest or southeast. The presence of a strong stratification of the density of the marine environment may prevent the plume from entering the near-surface layers. In this regard, the plume was not detected on every satellite multispectral image. With the smooth stratification of the marine environment, the wastewater jets reach the near-surface layers and form a local area of pollution with optical contrasts, which are detected on multispectral satellite images.

A joint analysis of Figures 7 and 10a,b made it possible to identify the areas of anthropogenic impacts due to submerged wastewater discharges, coinciding in a spatial position in the immediate vicinity of the outfall. These areas appeared in the fields of distribution of the significant parameters of the water environment (Figure 10a,b), generally coinciding with the location of the zone of the most frequent plume registration from multispectral images (see Figure 7, red and purple areas of the color-coded map).

In addition to the considered examples of a comprehensive analysis of the heterogeneous satellite and sea truth data processing results, an experiment which aimed at obtaining a quantitative estimate of the accuracy of the determination of the wastewater plume boundaries was carried out. To do this, we analyzed the results of numerous in situ measurements obtained during the shipboard operations, as well as the spatial and geometric characteristics of the plume recorded by the satellite methods in the same seasons. We used the results of the processing data from the shipborne measurements of the significant parameters of the water environment, presented as two-dimensional distributions (see, for example, Figures 7b and 10b), namely [34]:

- Temperature (°C, near-surface layer);
- Salinity (PSU, near-surface layer);
- Density (kg/m^3, near-surface layer);
- Salt Content (t/m^2, 1–25 m layer);
- Thermal Content (mJ/m^2, 1–25 m layer);
- pH (near-surface layer);
- Phosphate concentration (µmol/L, near-surface layer);
- Alkalinity (meq/L, near-surface layer);
- Ammonium concentration (µmol/L, near-surface layer);
- Turbidity (FTU, selected layer with maximum of turbidity);
- Light attenuation index (extinction rate) (1/m, selected layer with maximum of turbidity);
- Total Suspended Matter (TSM) (mg/L, near-surface layer);
- Total Inorganic Carbon (TIC) (µmol/L, near-surface layer).

Based on the study of the spatial distributions of these significant parameters of the water environment, according to the shipboard data the points that correspond to the maximum levels of the anthropogenic impacts of the deep plumes were located (see, e.g., Figure 10b, where the extrema are clearly visible and correspond to dark spots). A total of 103 such points were founded. Then, they were loaded into the geoinformational system and analyzed together with the results of the satellite data processing, as shown in Figure 11.

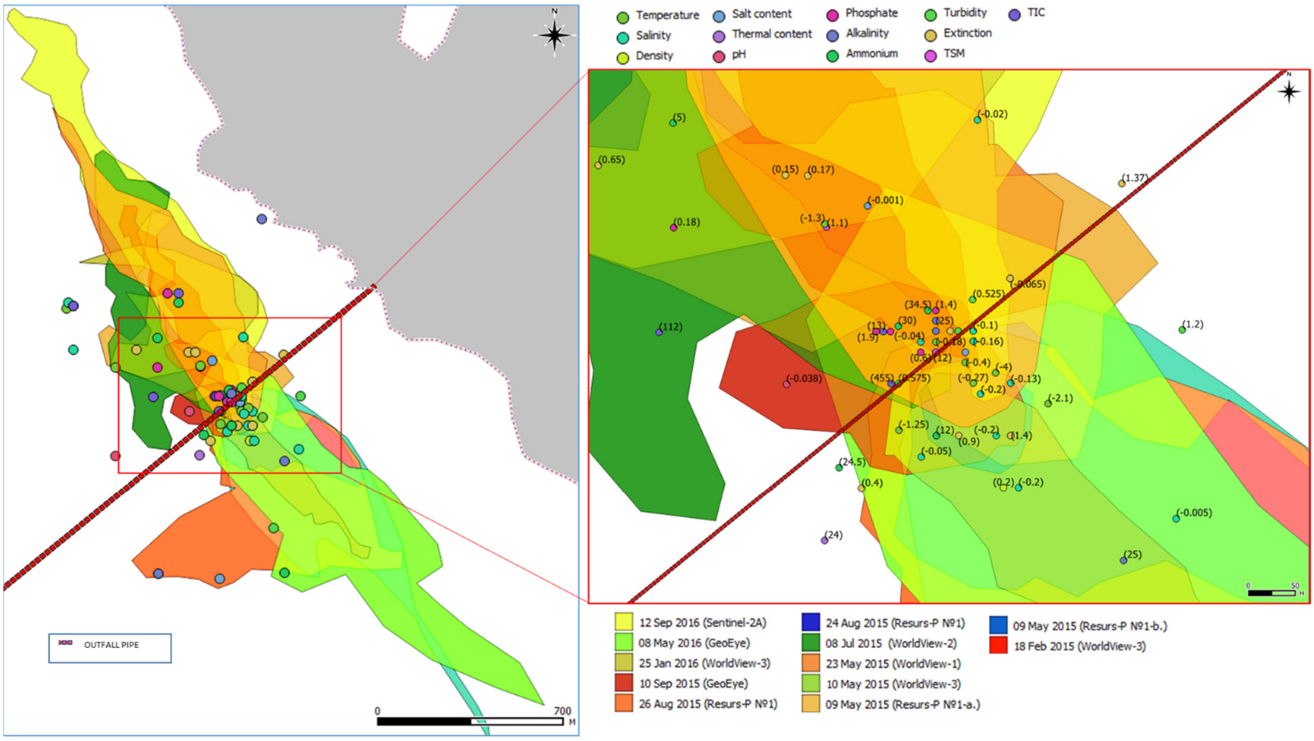

Figure 11. The schematic map illustrating the spatial position of the results of submerged plume detection according to satellite multispectral data (colored polygons) and the points of registered maximum levels of anomalies of the water environment's significant parameters according to sea truth measurements (colored circles) in the test area. Actual deviations of the measured parameters from the background values are given in brackets in the enlarged fragment.

An analysis of Figure 11 shows good correlation between the results of the satellite and sea truth data processing. Most of the points (over 84%) of the maximum levels of anthropogenic impacts, identified by the results of the in situ data processing, are located within the generalized contour of the wastewater plume, based on the processing of the satellite multispectral data. Thus, a quantitative approach was proposed and implemented to assess the adequacy of the generated satellite information products.

Summing up the comprehensive analysis of the results obtained, it should be noted that the various methods of satellite remote sensing and the methods for processing the optical and radar images made it possible to register various physical processes due to the anthropogenic impacts on coastal waters. The conducted research has shown, on the one hand, the variety of kinds of manifestation of anthropogenic impacts caused by submerged wastewater discharges on coastal waters and, on the other hand, a wide range of capabilities for recording and studying such manifestations by satellite methods. These capabilities are realized, first of all, by the relationship between the electromagnetic fields recorded by the satellite equipment, the spatial structure of the surface waves, and the optical characteristics of the near-surface layer of the water environment. The joint use and integration of the heterogeneous remote sensing data opens up broad prospects for versatile research and the control of anthropogenic impacts on coastal waters. In this case, the specialized data processing techniques should be used that take into account the physical features of the remote indication of the anthropogenic impacts on coastal waters, providing a correct interpretation of the observed changes in the significant parameters of the marine environment.

5. Conclusions

Remote sensing methods provide great opportunities for studying marine areas; however, the capabilities of these methods have not been studied in sufficient detail. The features of the satellite study of the intense anthropogenic impacts of submerged wastewater discharge on marine areas are summarized and analyzed in this article. The science behind the problem of revealing and investigating anthropogenic impacts due to submerged wastewater discharges by satellite methods is developed and updated. The results of the collection, systematization, processing, and analysis of the experimental satellite and sea truth data obtained in the northern part of the Black Sea in areas affected by submerged wastewater discharges are demonstrated and discussed. The following main conclusions can be drawn as a result of the work:

1. Based on the analysis of the current level of research in the field of the remote sensing of anthropogenic impacts on marine areas, the approaches were defined and tested for studying submerged wastewater discharges using the satellite data generated in different wavelength ranges of the electromagnetic spectrum, namely:
    - An approach based on the analysis of the spatial spectra of high- and medium-resolution (1–10 m) optical and radar satellite imagery;
    - An approach based on the registration of changes in a normalized radar cross-section due to sea waves using radar satellite imagery;
    - An approach based on the study of the spectral features of optical radiation reflected and scattered by the marine environment using medium-resolution optical data.
2. Spatial distributions of the surface manifestations of disturbances in the stratified water column (internal waves) caused by wastewater jets can be recorded using the methods of the spatial spectral analysis of high-resolution (~1 m) satellite images. At the same time, zones of anthropogenic impacts are detected by "quasi-monochromatic" maxima in the spatial spectra of fragments of optical and radar images, indicating the quasi-periodic structures on the sea surface that have spatial periods of the order of several decameters due to the interaction of short-period internal waves generated by deep discharge with the surface waves. New actual results have been obtained, confirming, among other things, the possibility of using radar data to study such effects, as well as the feasibility of generating and studying mosaics based on a long-term (annual) time series of satellite data of medium spatial resolution (~10 m).
3. All-weather satellite radars that record changes in the intensity of surface waves in the gravitational–capillary range provide the capability to identify the anthropogenic effects of wastewater discharges, resulting in deformations of surface waves by surfactant films, internal waves, and turbulence. The processing of medium-resolution radar satellite images made it possible to identify the zones of NRCS changes associated with deformations of the surface wave field, which are caused by the anthropogenic impacts caused by submerged discharge. The contrast values corresponding to "moderate" and "strong" anthropogenic impacts were ~2 dB and ~4 dB, respectively.
4. Numerous anomalies in the spectral radiance of the near-surface layer of the water environment, caused by submerged plumes, were identified based on the results of the processing of medium-resolution multispectral satellite images, and the geometric characteristics of plumes were determined. In the case when wastewaters are discharged to a quite shallow depth (~30 m) and often reach the surface and near-surface layers of the water column, medium-resolution multispectral satellite imagery is an effective tool for recording and studying the anthropogenic impacts. An experimental

testing of the proposed I_{GBnorm} color index was carried out, which allowed for a long period (from 2015 to 2021) research and analysis of the dynamics of the anthropogenic impact zones due to discharge plumes coming from a rupture in the outfall collector.

5. The data on the shape and location of the manifestation zones of submerged wastewater obtained by various methods (including sea truth) complement each other. The adequacy of the obtained results was confirmed by a comprehensive analysis of the heterogeneous (including sea truth) data using geoinformational technologies.

Author Contributions: Conceptualization, V.B.; methodology, V.B. and V.Z.; software, V.Z.; formal analysis, V.B. and V.Z.; investigation, V.B. and V.Z.; data curation, V.Z.; writing—original draft preparation, V.Z.; writing—review and editing, V.B.; visualization, V.Z.; supervision, V.B. All authors have read and agreed to the published version of the manuscript.

Funding: This work was carried out under the financial support of the Ministry of Science and Higher Education of the Russian Federation within the framework of Agreement # 075-15-2020-776.

Institutional Review Board Statement: Not applicable.

Informed Consent Statement: Not applicable.

Data Availability Statement: Not applicable.

Conflicts of Interest: The authors declare no conflict of interest.

References

1. Israel Yu, A.; Tsyban, A.B. *Ocean Anthropogenic Ecology*; Flinta: Moscow, Russia, 2009; p. 529. (In Russian)
2. Roberts, P.J.W. Sea Outfalls. In *Environmental Hydraulics Water Science and Technology Library*; Singh, V.P., Hager, W.H., Eds.; Springer: Dordrecht, The Netherlands, 1996; pp. 63–110.
3. Bondur, V.G. Aerokosmicheskie Metody v Sovremennoy Okeanologii (Aerospace Methods in Modern Oceanology). In *New Ideas in Oceanology*; Nauka: Moscow, Russia, 2004; pp. 55–117.
4. Bondur Valery, G. Satellite Monitoring and Mathematical Modelling of Deep Runoff Turbulent Jets in Coastal Water Areas. In *Waste Water Evaluation and Management*; InTech: Rijeka, Croatia, 2011; pp. 155–180. ISBN 978-953-307-233-3. [CrossRef]
5. Seegers, B.N.; Teel, E.N.; Kudela, R.M.; Caron, D.A.; Jones, B.H. Glider and remote sensing observations of the upper ocean response to an extended shallow coastal diversion of wastewater effluent. *Estuar. Coast. Shelf Sci.* **2017**, *186*, 198–208. [CrossRef]
6. Bondur, V.G.; Grebenuk, Y.V. Remote indication of anthropogenic influence on marine environment caused by depth wastewater plume: Modelling, experiments. *Issled. Zemli Kosm.* **2001**, *6*, 49–67.
7. Bondur, V.G.; Zhurbas, V.M.; Grebenyuk, Y.V. Mathematical modeling of turbulent jets of deep-water sewage discharge into coastal basins. *Oceanology* **2006**, *46*, 757–771. [CrossRef]
8. Kochergin, S.V.; Fomin, V.V. Variational identification of input parameters in the model of distribution of the pollutants from the underwater source. *Phys. Oceanogr.* **2019**, *26*, 547–556. [CrossRef]
9. Bondur, V.G.; Keeler, R.N.; Starchenkov, S.A.; Rybakova, N.I. Monitoring of the pollution of the ocean coastal water areas using space multispectral high resolution imagery. *Issled. Zemli Kosm.* **2006**, *6*, 42–49.
10. Bondur, V.G.; Vorobjev, V.E.; Grebenjuk, Y.V.; Sabinin, K.D.; Serebryany, A.N. Study of fields of currents and pollution of the coastal waters on the Gelendzhik shelf of the Black Sea with space data. *Izv. Atmos. Ocean. Phys.* **2013**, *49*, 886–896. [CrossRef]
11. Bondur, V.G.; Zubkov, E.V. Vydelenie melkomasshtabnykh neodnorodnostey opticheskikh kharakteristik verkhnego sloya okeana po mnogozonalnym sputnikovym izobrazheniyam vysokogo razresheniya. Chast 1. Effekty sbrosa drenazhnykh kanalov v pribrezhnye akvatorii (Showing up the small-scale ocean upper layer optical inhomogeneities by the multispectral space images with the high surface resolution. Part 1. The canals and channels drainage effects at the coastal zone). *Issled. Zemli Kosm.* **2005**, *4*, 54–61.
12. DiGiacomo, P.; Washburn, L.; Holt, B.; Jones, B.H. Coastal pollution hazards in southern California observed by SAR imagery: Stormwater plumes, wastewater plumes, and natural hydrocarbon seeps. *Mar. Pollut. Bull.* **2004**, *49*, 1013–1024. [CrossRef]
13. Bondur, V.G.; Zamshin, V.V. Comprehensive Ground-Space Monitoring of Anthropogenic Impact on Russian Black Sea Coastal Water Areas. In *Scientific-Practical Conference "Research and Development—2016"*; Anisimov, K.V., Dub, A.V., Kolpakov, S.K., Lisitsa, A.V., Petrov, A.N., Polukarov, V.P., Popel, O.S., Vinokurov, V.A., Eds.; Springer International Publishing: Cham, Switzerland, 2018; pp. 625–637. [CrossRef]
14. Gierach, M.M.; Holt, B.; Trinh, R.; Pan, B.J.; Rains, C. Satellite detection of wastewater diversion plumes in Southern California. *Estuar. Coast. Shelf Sci.* **2017**, *186*, 171–182. [CrossRef]
15. Ivanov, A.Y. Slicks and Oil Films Signatures on Syntetic Aperture Radar Images. *Issled. Zemli Kosm.* **2007**, *3*, 73–96. (In Russian)

16. Pugach, S.P.; Pipko, I.I.; Shakhova, N.E.; Shirshin, E.A.; Perminova, I.V.; Gustafsson, Ö.; Bondur, V.G.; Ruban, A.S.; Semiletov, I.P. Dissolved organic matter and its optical characteristics in the Laptev and East Siberian seas: Spatial distribution and interannual variability (2003–2011). *Ocean Sci.* **2018**, *14*, 87–103. [CrossRef]
17. Trinh, R.C.; Fichot, C.G.; Gierach, M.M.; Holt, B.; Malakar, N.K.; Hulley, G.; Smith, J. Application of Landsat 8 for Monitoring Impacts of Wastewater Discharge on Coastal Water Quality. *Front. Mar. Sci.* **2017**, *4*, 329. [CrossRef]
18. Bondur, V.G.; Zamshin, V.V.; Zamshina, A.S.; Vorobyev, V.E. Registering from Space the Features of Deep Wastewater Outfalls into Coastal Water Areas Due to Discharge Collector Breaks. *Izv. Atmos. Ocean. Phys.* **2020**, *56*, 979–988. [CrossRef]
19. Alpers, W.; Zhang, B.; Mouche, A.; Zeng, K.; Chan, P.W. Rain footprints on C-band synthetic aperture radar images of the ocean—Revisited. *Remote Sens. Environ.* **2016**, *187*, 169–185. [CrossRef]
20. Solberg, A.H.S.; Brekke, C.; Husoy, P.O. Oil Spill Detection in Radarsat and Envisat SAR Images. *IEEE Trans. Geosci. Remote Sens.* **2007**, *45*, 746–755. [CrossRef]
21. Optika Okeana (Ocean Optics). In *Fizichekaya Optika Okeana (Physical Ocean Optics)*; Monin, A.S., Ed.; Nauka: Moscow, Russia, 1983; Volume 1, pp. 208–234.
22. Brando, V.E.; Anstee, J.M.; Wettle, M.; Dekker, A.G.; Phinn, S.R.; Roelfsema, C. A physics based retrieval and quality assessment of bathymetry from suboptimal hyperspectral data. *Remote Sens. Environ.* **2009**, *113*, 755–770. [CrossRef]
23. Pratt, W.K.; Collins, D. *Digital Image Processing*; Wiley: New York, NY, USA, 1978; 776p.
24. Cormen, T.H.; Leiserson, C.E.; Rivest, R.L.; Stein, C. *Introduction to Algorithms*, 4th ed.; The MIT Press: Cambridge, MA, USA, 2022; 1291p.
25. Nyquist, H. Certain Topics in Telegraph Transmission Theory. *Cond. Affect. Success Main Line Electrif.* **1928**, *47*, 617–644. [CrossRef]
26. ESA European Space Agency Missions, Sentinel-2 [Electronic Resource]. Available online: https://sentinels.copernicus.eu/web/sentinel/missions/sentinel-2 (accessed on 22 June 2021).
27. ESA European Space Agency Missions, Sentinel-1 [Electronic Resource]. Available online: https://sentinels.copernicus.eu/web/sentinel/missions/sentinel-1 (accessed on 22 June 2021).
28. *Landsat 8 (L8) Data Users Handbook*, 5th ed.; USGS: Reston, VA, USA, 2019; 114p.
29. Jackson, C.; Apel, J. (Eds.) *SAR Marine Users Manual*; NOAA: Washington, DC, USA, 2004; 464p. Available online: https://www.star.nesdis.noaa.gov/socd/mecb/sar/PUBLICATIONS/SARUsersManual/NOAA_SARMarineUsersManual_Dec2004.pdf (accessed on 8 August 2022).
30. Brekke, C.; Solberg, A.H. Oil spill detection by satellite remote sensing. *Remote Sens. Environ.* **2005**, *95*, 1–13. [CrossRef]
31. Ivanov, A.Y.; Zatyagalova, V.V. A GIS approach to mapping oil spills in a marine environment. *Int. J. Remote Sens.* **2008**, *29*, 6297–6313. [CrossRef]
32. O'Reilly, J.E.; Werdell, P.J. Chlorophyll algorithms for ocean color sensors—OC4, OC5 & OC6. *Remote Sens. Environ.* **2019**, *229*, 32–47. [CrossRef]
33. Robinson, I.S. *Discovering the Ocean from Space: The Unique Applications of Satellite Oceanography*; Springer: Berlin/Heidelberg, Germany, 2010; 638p.
34. Bondur, V.G.; Ivanov, V.A.; Vorobiev, V.E.; Dulov, V.; Dolotov, V.V.; Zamshin, V.V.; Kondratiev, S.I.; Lee, M.E.; Malinovsky, V.V. Ground-to-Space Monitoring of Anthropogenic Impacts on the Coastal Zone of the Crimean Peninsula. *Phys. Oceanogr.* **2020**, *27*, 95–107. [CrossRef]